

NBSIR 74-628

**Mass Transport and Physical Properties of
Large Crystals of Calcium Apatites:
Studies of $\text{Ca}(\text{OH})_2$ Crystals For Use in
Electrolytic Conversion of Calcium Fluorapatite
Crystals to Calcium Hydroxyapatite**

A. D. Franklin and K. F. Young

Inorganic Materials Division
Institute for Materials Research
National Bureau of Standards
Washington, D. C. 20234

September 1, 1973 – August 31, 1974

Annual Report II

Prepared for
**Department of Health, Education, and Welfare
National Institutes of Health
National Institute of Dental Research
Bethesda, Md. 20014**
Interagency Agreement No. Y01-DE-30010

NBSIR 74-628

**MASS TRANSPORT AND PHYSICAL PROPERTIES OF
LARGE CRYSTALS OF CALCIUM APATITES:
STUDIES OF $\text{Ca}(\text{OH})_2$ CRYSTALS FOR USE IN
ELECTROLYTIC CONVERSION OF CALCIUM FLUORAPATITE
CRYSTALS TO CALCIUM HYDROXYAPATITE**

A. D. Franklin and K. F. Young

Inorganic Materials Division
Institute for Materials Research
National Bureau of Standards
Washington, D. C. 20234

September 1, 1973 – August 31, 1974

Annual Report II

Prepared for
Department of Health, Education, and Welfare
National Institutes of Health
National Institute of Dental Research
Bethesda, Md. 20014

Interagency Agreement No. Y01-DE-30010



U. S. DEPARTMENT OF COMMERCE

NATIONAL BUREAU OF STANDARDS, Richard W. Roberts, Director

ABSTRACT

In order to convert single crystals of calcium fluorapatite to calcium hydroxyapatite, an electrolytic cell technique will be explored. To utilize such a technique, the cathode compartment must consist of a source of hydroxyl ions and a barrier to the flow of all others. Ca(OH)_2 has been selected for the cathode material, backed by a Pt electrode in an atmosphere containing H_2O and O_2 . Ca(OH)_2 crystals have been grown and Ag as well as Pt electrodes applied to them. Their ac admittance as a function of temperature has been measured and analyzed. A Warburg contribution to the admittance was observed to depend upon the presence of O_2 . Equivalent circuits have been generated from the data allowing us to tentatively characterize the electrical properties of the electroded crystal system.

1. INTRODUCTION

We propose to electrolytically convert available large crystals of either calcium fluorapatite ($\text{Ca}_{10}(\text{PO}_4)_6\text{F}_2$, or FAp) or calcium chlorapatite ($\text{Ca}_{10}(\text{PO}_4)_6\text{Cl}_2$, or ClAp) to calcium hydroxyapatite ($\text{Ca}_{10}(\text{PO}_4)_6(\text{OH})_2$ or OHAp). In their closely related crystal structures¹, the X^- ions in XAp are known to be relatively mobile.² Possibly, then, large crystals of OHAp can be prepared by replacing F^- in FAp or Cl^- in ClAp crystals by OH^- .

Young and Elliot³ have replaced all but 6% of the Cl^- with OH^- ions in ClAp by using the diffusion controlled process of annealing ClAp in steam at 1000°C. This would take an almost infinite amount of time to replace the last traces of Cl^- ions with OH^- ions, whereas an electrolytic technique would drive out the X^- ions and drive in the OH^- ions at a steady rate determined by the magnitude of the impressed current.

It is, therefore, the first objective of this project to test the possibility of the electrochemical transformation of large single crystals of FAp to OHAp.

This is to be accomplished by constructing a solid electrolytic cell of Pt:CaF₂:FAp:Ca(OH)₂:Pt. For the anode compartments, it has been shown that the transport number of F^- ions in CaF₂ is unity⁴ and the conductivity of oxygen-doped CaF₂ is sufficient for the desired current to flow. For the cathode compartment, we have chosen Ca(OH)₂ as the most likely candidate for the OH^- ion conductor. We have diffusion-grown crystals suitable for characterizing OH^- ionic conduction, but work is continuing on an electrolytic growth technique which should produce larger crystals needed ultimately for making sizeable OHAp crystals using the electrolytic conversion cell.

Silver paint electrodes were used on some specimens and made possible electrical measurements that seem to hold out promise for characterization Ca(OH)₂. These data shows a Warburg dependence of the electrode-specimen interface which we interpret as a diffusion-controlled blocking process. The next step, then, is to experiment with the electrodes which

eliminate this blocking to allow measurement of the bulk conduction of Ca(OH)_2 and which ultimately we can use in the electrolytic conversion cell.

2. CRYSTAL GROWTH

Crystals of Ca(OH)_2 suitable for most of the studies planned have been grown by the diffusion technique described in the last Annual Report. Ultimately, however, it will be desirable to have larger crystals. The diffusion technique is limited in the apparent crystal size produced, at least in small vessels. Once the original charge of CaCl_2 and NaOH have reacted, there appears to be no way to add new reactants without nucleating new crystals. What is needed is a way to draw continuously and slowly from large reservoirs of reactant as growth proceeds.

Some experiments have been performed on a possible new technique to do this, utilizing an electric current through an ionic solution as a way to move ions from one compartment to another. This technique is illustrated by the sketch in Fig. 1 of one experimental apparatus. A U-tube contains agar-agar made with 1 M KI solution so that liquid cannot pass freely between the arms of the tube. A solution of KI (1 M), and CaCl_2 (0.1 M) (slightly acidified to minimize CO_2) is placed in the cathode and anode compartments. The cathode compartment also contains a stirring device and a probe to monitor the resistance of the solution.

A small current, of the order of 1 mA, is then passed continuously through the cell. At the cathode H_2O is decomposed, forming H_2 gas and OH^- ions. At the anode, I^- ions discharge, most reacting with the OH^- ions to release O_2 gas and form H_2O . The overall reaction is the formation of OH^- ions in the cathode, and their disappearance in the anode compartments. Because of the large concentration of "inert" ions (K^+ and I^-) there is probably little or no electric field in the bulk of the cell. Thus, the concentration of OH^- ions builds up in the cathode compartment and decreases in the anode compartment until a diffusion flux is created transporting OH^- ions from cathode to anode.

At the same time depletion of the OH^- ions concentration in the anode compartment will cause the dissolution of some of the Ca(OH)_2 in contact with the electrolyte in that compartment. As a result,

the Ca^{2+} ion concentration will be increased in the anode compartment and a diffusion flux will carry Ca^{2+} ions toward the cathode compartment. At steady state, the total current will be carried by the sum of the OH^- and Ca^{2+} fluxes. By controlling the current, the magnitude of these fluxes can be controlled, and hence, the value of the concentrations of each ion in the two compartments. If the current be properly adjusted, the solubility of $\text{Ca}(\text{OH})_2$ can be exceeded in the cathode compartment and $\text{Ca}(\text{OH})_2$ made to crystallize there. The result is a continuous transfer of $\text{Ca}(\text{OH})_2$ from the anode to the the cathode compartments, at a rate determined by the easily-controllable current.

In principle the transport equations governing the flow of mass and charge in this system can be set-up and solved and the time dependence of concentrations determined in the various compartments, at least for simplified geometries. This analysis has been started but not yet completed. However, in a qualitative way the steady-state behavior expected can be understood in terms of Fig. 2, drawn for the situation in which the initial concentration of Ca^{2+} greatly exceeds that of OH^- . At zero time both would be represented by the horizontal dotted line at unit relative concentration.

If the $\text{Ca}(\text{OH})_2$ layer were not present, or if the dissolution of the $\text{Ca}(\text{OH})_2$ were very slow compared to the discharge of ions at the electrodes, then the OH^- ion concentration would rise in the cathode compartment and fall in the anode compartment until a concentration gradient was established such that the charge transported by the diffusion flux of the OH^- ions just equaled the current in the external circuit. At the same time $\text{Ca}(\text{OH})_2$ would precipitate in the cathode compartment until the Ca^{2+} ion concentration in the entire cell became uniform at the value dictated by the solubility product and the OH^- ion concentration in the cathode compartment. No more precipitation of $\text{Ca}(\text{OH})_2$ would take place, and no more charge transport by Ca^{2+} ion. The entire current in the cell would be carried by OH^- ions.

With Ca(OH)_2 dissolving from the reservoir at a finite rate, some of the OH^- ions reaching the anode would be provided by this process and fewer by diffusion in the agar-agar layer. The negative concentration gradient of OH^- ions in this layer would be correspondingly lower. The Ca^{2+} ion concentration in the anode compartment and in the Ca(OH)_2 layer would be increased, giving rise to a negative concentration gradient of Ca^{2+} ions in the agar-agar layer and a flux of these ions into the cathode compartment where they would react with some of the OH^- ions produced at the cathode and precipitate as Ca(OH)_2 . Hence some of the current in the bulk of the cell would be carried by the Ca^{2+} ions flowing counter to the OH^- ions. The proportion carried this way will depend upon the rates of dissolution and precipitation of Ca(OH)_2 and of diffusion of Ca^{2+} and OH^- ions. In the limit of very fast dissolution and Ca^{2+} transport, all of the current would be carried by Ca^{2+} ions, and the net result would be the quantitative transport of Ca(OH)_2 from the reservoir to the cathode compartment. The actual situation probably lies somewhere between the two extremes of transport purely by OH^- or Ca^{2+} ions.

A number of experiments have been performed to test these general ideas. In one set of experiments a simplified apparatus consisting of two concentric tubes with a hole in the inner joining the two was used. No reservoir of Ca(OH)_2 was provided, and the solution contained 1M KCl plus 0.1 M CaCl_2 . Crystal plates of Ca(OH)_2 several mm across were grown on Cu and brass cathodes, demonstrating the feasibility of the technique. The lack of the Ca(OH)_2 reservoir, however, precluded extended growth.

In a second set of experiments, the configuration of Fig. 1 was used, with CaCl_2 added to the cathode compartment only. Crystal growth on the cathode has again been observed, as well as general precipitation in the cathode compartment. The transport of Ca(OH)_2 from the reservoir into the cathode compartment has been demonstrated but more experiments are needed to find the conditions of concentration and current required to give smooth crystal growth without excessive nucleation.

3. ELECTRODE APPLICATION

The electrodes in these experiments need to act both as catalysts and as electron transfer agents to ensure an adequate supply of hydroxyl ions. For this purpose the electrodes must be porous enough for rapid diffusion of atmospheric H_2O and O_2 to the sites where OH^- ions can be formed and transferred to the crystal. Without sufficiently porous electrodes capable of sufficiently rapid adsorption and catalytic formation of OH^- ions, the obtainable current may be limited by the diffusion and catalytic processes rather than by mass transport in the crystal. This kind of situation has been studied recently for stabilized zirconia solid electrolytes with Pt electrodes in various atmospheres^{5, 6}.

Evaporation was tried as the first technique for putting down Pt electrodes. The initial experiments, as reported in our last Annual Report, were encouraging. Additional experiments during this past year showed that the crystals could be handled in air with reasonable precautions without measurable weight gain, and that carbonate layers that did form from long exposure to air at room temperature appeared to do so only on the surface, even when the crystal turned quite milky and opaque. A 2% HNO_3 solution etched this layer rapidly, leaving a clear crystal that dissolved only very slowly.

Under the heating from the filament in the vacuum the crystals sometimes were damaged, probably by loss of H_2O . The resulting crystal was milky rather than clear and cleaved into numerous milky slices along the basal planes. To avoid the overheating a jig was built as shown in Fig. 3. Two removable radiation shields protected the sample and holder from all but the part of the filament bearing the evaporating Pt. The jig is made of brass and soft-soldered to a copper plate to which copper tubing is soldered for water-cooling. A heating element in the base of the jig allows the temperature to be raised in a controlled fashion for out-gassing, and a thermocouple reaching into the center of the jig just below the specimen holder monitors the jig temperature.

In order to ensure as smooth and controlled evaporation as possible, the tungsten supports with the Pt are cleaned with hot concentrated NaOH followed by distilled H₂O, and not touched except with tweezers subsequently. Spiral tungsten baskets with 10-30 mg of Pt were found to be preferable to tungsten loops or "hair-pins". With the latter the Pt tended to form discrete drops, undoubtedly as a result of effects arising from the temperature dependence of the surface tension. When this happened the filament was prone to burn out in the thin regions between drops before much of the Pt evaporated.

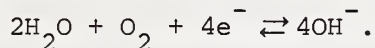
With these arrangements it has been possible to deposit good mirrors on a glass tube set beside the specimen jig in the vacuum, but not to produce entirely satisfactory films on the specimens. The films that were deposited tended to flake off readily and to be quite coarse in comparison to the mirrors on the glass.

Possible problems are: 1) the size of the apertures in the radiation shields, which may be too small; 2) the use of benzene to protect the crystal, since a surface film may be left behind; 3) slow decomposition of the crystal itself, producing enough H₂O vapor to interfere with the deposition of Pt atoms on the crystal surface. Experiments with the evaporation will continue to try to determine the cause of poor films. At the same time, arrangements have been made to sputter Pt films using equipment in another laboratory to see if this rather different technique, involving essentially no heat, can produce better films.

Initially, the Pt electrodes were evaporated onto as-grown crystals which were about (10) mm² in area and about (1) mm thick. This small area to thickness ratio of the two electroded surfaces yielded low specimen capacitance. However, attempts to cleave the crystals were very successful and thickness of the specimen could be reduced by approximately a factor of 10. For measuring the capacitance of these latest specimens we used silver paint electrodes. These electrodes were not expected to provide satisfactory catalysts for exchange with the atmosphere but were intended only as an expedient means in our

efforts to improve the signal-to-noise ratio of our electrical measurements. However, the data indicated the expected dependence upon the presence of oxygen in the specimen environment. This data is analyzed in the next section (electrical measurements) although these silver paint electrodes are not well characterized.

We must have electrodes which will catalyze the reaction



They must also be porous enough so that the reactants may diffuse through to the double interface of solid-solid-gas [Pt-Ca(OH)₂-Reactant gas.] A thin ($\sim 300\text{\AA}$) film of platinum, either evaporated or sputtered, should fulfill these requirements best. The porosity, thickness, and impurities of the silver paint electrodes which were used for developing the measurement techniques are unknown and are probably not ideal. However, increases in the equivalent circuit parameters generated from the data correlate well with the increases of the partial pressure of oxygen, suggesting some catalytic activity.

4. ELECTRICAL MEASUREMENTS

The apparatus which was described in earlier reports had considerable shunt capacitance relative to the very small capacitance of the specimen. Measurements were made for specimens of CaF₂ with known low capacitance and also for "blank runs", i. e., no specimen in place. The shunt capacitance was reduced from 0.23 pF to <0.08 pF by placing electrically shielding stainless steel tubing and sheet between the lead and probes within the environmental chamber. Hence, this capacitance to ground is not included in the measurement and greatly improves our "signal-to-noise" ratio.

The capacitance of a disc-shaped specimen varies as the inverse of the thickness of the disc. Therefore, thinner specimens have a larger capacitance and improve our measuring ability by increasing the ratio of sample capacitance to background (or shunt) capacitance. Our cleaved specimens are thinner than as-grown crystals by approximately a factor of 5. This increased sample capacitance along with the decreased shunt capacitance yield the following overall improvement. With the shielded specimen holder and thicker uncleaved specimens, we measured 0.23 pF shunt capacitance and estimated the sample capacitance to be 0.15 pF.

With the improved shielding and thinner specimens, we measure 0.85 pF for the sample and estimate shunt values to be <0.08 pF.

When mass transfer impedance is governed by diffusional processes, there will be a contribution to the impedance that has an $\omega^{-1/2}$ dependence, where ω is the circular frequency. This is called a "Warburg impedance", Z_w^* , (see Sluyters-Rehback and Sluyters⁷). Typically, in measurements on KHF_2 Bruinink and Broers⁸ show this by simultaneously plotting measured values of conductance versus $\omega^{1/2}$ and capacitance versus $\omega^{-1/2}$. If Warburg behavior exists, then there should be linear regions with the same slope for each curve. This is so because,

$$Z_w^* = (1-j)\sigma \omega^{-1/2}$$

and

$$Y_w^* = (1+j) \frac{1}{2\sigma} \omega^{1/2} = G + j\omega C.$$

Equating real and imaginary parts,

$$G = \frac{1}{2\sigma} \omega^{1/2}$$

$$C = \frac{1}{2\sigma} \omega^{-1/2}$$

We expected our porous electroded specimens to exhibit this behavior and, indeed, as shown in Fig. 4 the linear central regions of the G and C curves have equivalent slopes for the corresponding partial pressures of O_2 .

It appears that we can also qualitatively account for the deviations from the Warburg behavior. For frequencies under 1 k Hz both the capacitance and conductance deviates somewhat from Warburg linearity; above 20 k Hz the conductance deviates significantly whereas the capacitance does so only slightly.

For low frequencies, the time period taken for one oscillation of the applied electric field becomes comparable to the time taken for the ionic species to diffuse a length equal the electrode thickness. If this is true, then as the frequency decreases there must be a transition to a Debye relaxation region which would have an equivalent circuit of a parallel resistance and capacitance. We call these resistance and capacitance parameters R_w and C_w , respectively. This situation is similar to that commonly observed when majority carriers are blocked at an electrode but minority carriers can be discharged. There is then a transition from high-frequency Warburg Behavior to low-frequency effects dominated by a parallel conductance-capacitance combination.

At high frequencies our measurement errors become too large for us to be certain of a Warburg dependence. However, the conductance cannot increase indefinitely and, indeed, it tends in our data to level off somewhat, as it must. Further, the capacitance at very high frequencies should extrapolate to something like the geometric capacitance of the specimen and our data show this behavior.

We can generate equivalent circuits for our specimen from these data, keeping in mind the change in the nature of the diffusional impedance as the frequency varies from high to low. The high frequency extrapolation of a C versus $\omega^{-1/2}$ curve gives us a shunt capacitance which we denote by C_g . This is most simply explained as the geometric capacitance of the plane parallel disc-shaped electrodes separated by the $\text{Ca}(\text{OH})_2$ specimen, although this may not be distinguishable from a double-layer capacitance at the electrodes in these data. Since all of our data behave this way, the shunt element, C_g , must appear in both equivalent circuits, shown in Fig. 5a and b.

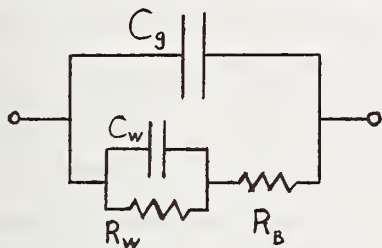


Fig. 5a. Low frequency

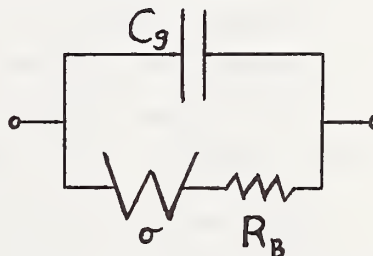


Fig. 5b. Mid-to-high frequency

As the frequency decreases below the Warburg region, the tendency toward larger G and a lower C is consistent with the transition of the diffusional impedance to a parallel network of R_w and C_w shunted by C_g . This is shown in Fig. 5a. In the mid-to-high-frequencies range we see a Warburg element shunted by the capacitance C_g as shown in Fig. 5b. At high frequencies the apparent bending over of the conductance curve is consistent with some bulk resistance, R_B , in series with the Warburg element. However, we cannot tell if C_g is shunting just R_B or the Warburg in series with R_B as shown, because R_B is apparently very small and our measuring precision at high frequencies is not good enough to distinguish between these possibilities.

There is another way to show that the Warburg dependence is obeyed at mid-frequencies and the data are at least consistent with Fig. 5b at high frequencies. That way is to plot the complex admittance, Y_w^* , of the presumed Warburg element, where according to our model,

$$Y_w^* = [Y^*]_m - Y_G^* = \left[(1+j) \frac{1}{2\sigma} \omega^{1/2} + j\omega C_g \right]_m - j\omega C_g$$

$$Y_w^* = (1+j) \frac{1}{2\sigma} \omega^{1/2}$$

where

$[Y^*]_m$ = measured complex admittance = $G+j\omega C$.

C_g = high frequency extrapolated geometric capacitance for that particular trial or measurement.

$Y_w^* = Y'_w + jY''_w$ is shown in the complex plane in Fig. 6. The plot exhibits the slope of unity for both the mid and high frequency ranges.

These electrical measurements are dependent upon the specimen's environment when the proposed diffusional processes do occur. Figures 4 and 6 show four consecutive trials all measured at 365°C where the atmosphere surrounding the specimen was varied between pure N_2 and a 4:1 mixture of $N_2:O_2$. The values obtained for the parameters $(2\sigma)^{-1}$, R_w^{-1} , C_w and C_g and are listed in Table I. The slopes of the plots of G and C against frequency (Fig. 4) yield values for $(2\sigma)^{-1}$, which show a reproducible increase when O_2 is introduced. The low frequency conductance, R_w^{-1} , also shows approximately the same increase whereas C_w and C_g show little or no effect. The expected effect of the presence of O_2 on the admittance parameters is encouraging. It suggests that OH^- ions are conducting and are exchanging with the atmosphere. Further, the apparently very small value for the bulk resistance, if real, means that the transport of OH^- ions may be as high as desired. Future experiments must measure R_B , however.

5. DISCUSSION

The analysis described here seems to fit the data taken so far, and indicates the direction to proceed with the studies. The strong frequency dependences observed arise from limiting reactions occurring at the electrode-electrolyte interfaces. The OH^- ions may "pile up" at

the $\text{Ca}(\text{OH})_2$ side of the interface so that the low frequency conductivity of the bulk is screened, in which case C_g is probably a space-charge capacitance. In addition, the Warburg impedance implies that diffusion of reactants through the electrodes is very slow. Our ultimate aim is to remove this limitation on OH^- transport imposed by these processes, so that the DC conductance coincides with R_B . That is, the experimental problem involves electroding processes and the observational criterion is the raising of the low-frequency portion of the conductance curve. The limiting factor is the catalyzed exchange with the atmosphere, so we need further work on the porous Pt electrodes, or possibly on other catalytically active materials.

REFERENCES

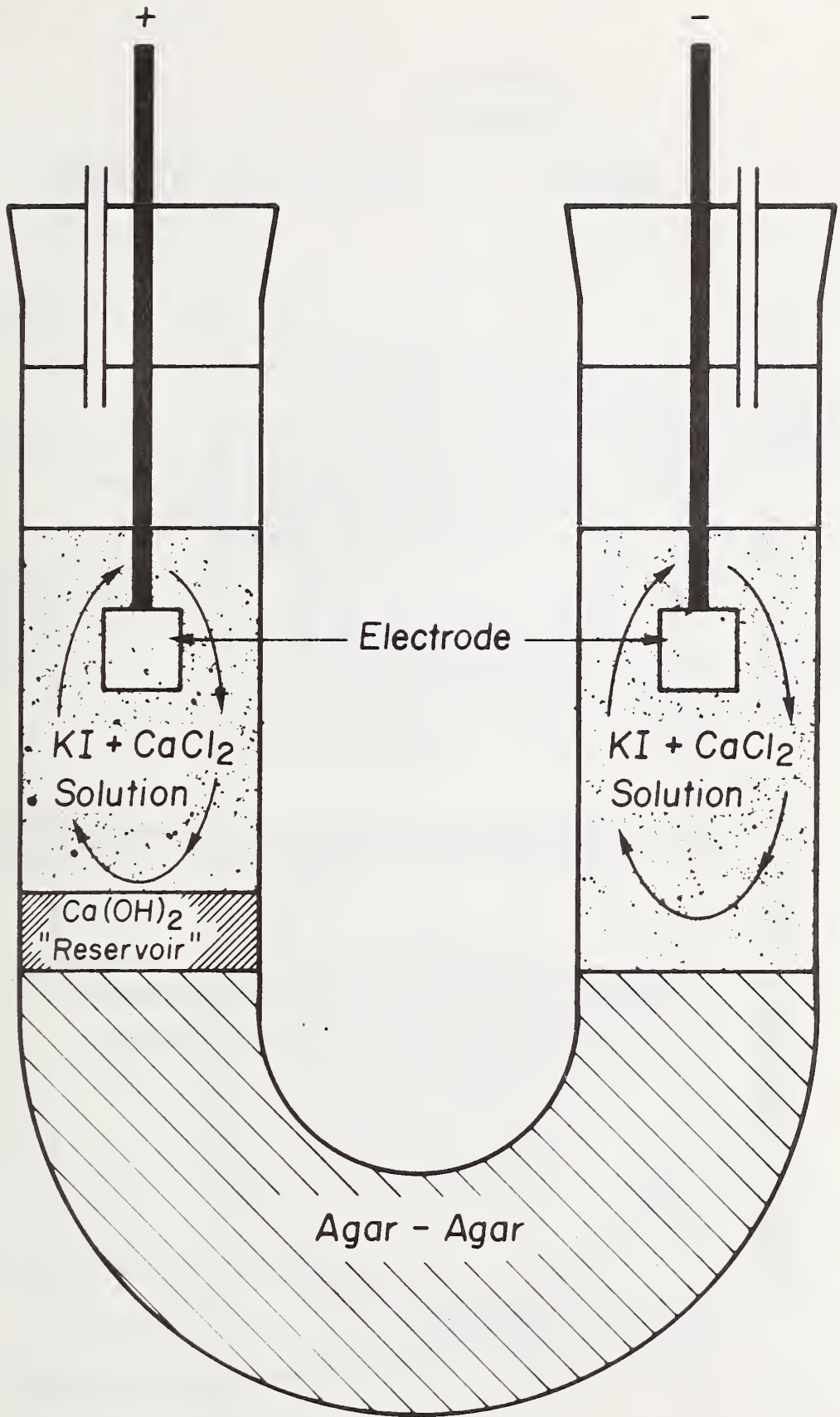
1. R. A. Young, *Trans. N. Y. Acad. Sci., Ser. II*, 29, 949 (1967).
2. C. Tse, D. O. Welch, and B. S. H. Royce, *Bull. Am. Phys. Soc., Ser. II*, 17, 265 (1972).
3. R. A. Young, and J. C. Elliott, *Arch. Oral Biol.*, 11, 699 (1966).
4. J. W. Hinze and J. W. Patterson, *J. Electrochem. Soc.*, 120, 96 (1973).
5. R. J. Brook, W. L. Pelzmann, and F. A. Kroger, *J. Electrochem. Soc.*, 118, 185 (1971).
6. T. H. Etsell and S. N. Flengas, *J. Electrochem. Soc.* 118, 1890 (1971).
7. M. Sluyters-Rehbach and J. H. Sluyters, *Electroanalytical Chemistry* ed. A. J. Bard (Marcel Dekker, Inc., New York, 1979), Vol. 4, p.16.
8. J. Bruinink and G. J. H. Broers, *J. Phys. Chem. Solids*, 33, 1713 (1972).
9. J. R. MacDonald, *J. Chem. Phys.*, 54 2026 (1971).

TABLE I

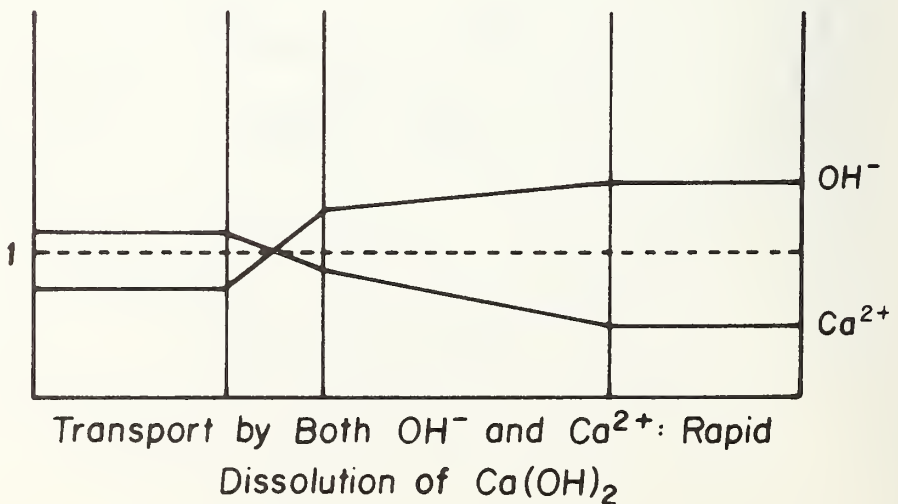
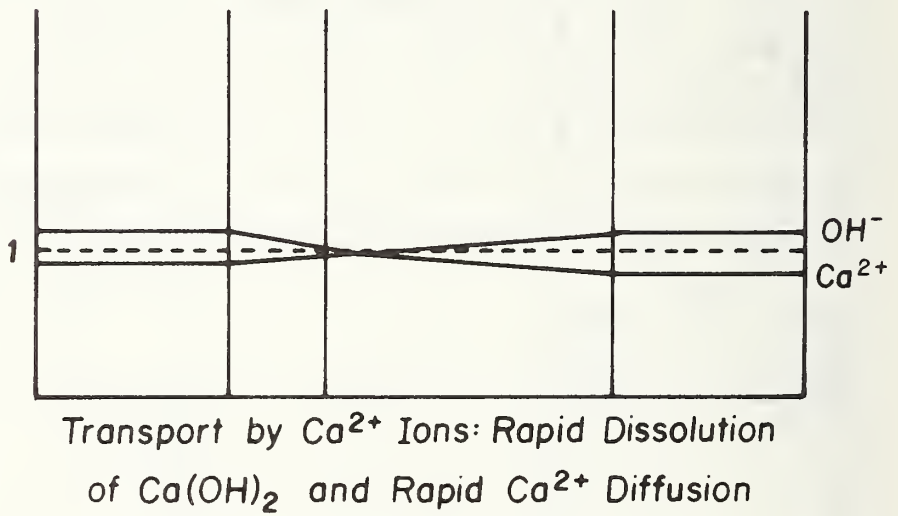
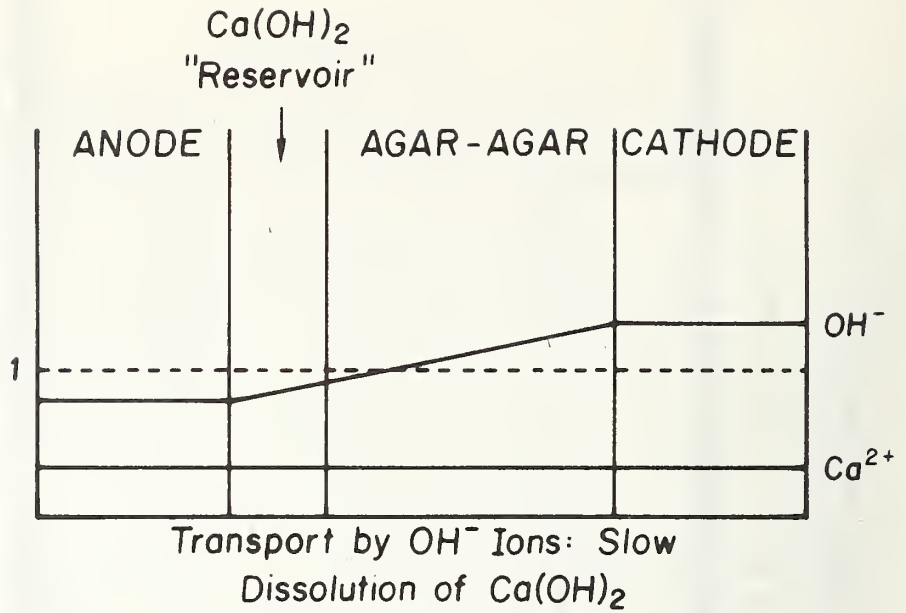
Environmental Atmosphere	$(2\sigma)^{-1}$	R_w^{-1}	C_w	C_g
	$\times 10^{-11}$ Siemens $\text{sec}^{-1/2}$ or Farads $\text{sec}^{1/2}$	$\times 10^{-10}$ Siemens	pF	pF
N ₂ :O ₂ , 4:1	1.90	6.5	.6 ± .1	.853
N ₂ only	1.76	5.7	"	.855
N ₂ :O ₂ , 4:1	1.88	7.6	"	.859
N ₂ only	1.64	5.7	"	.861

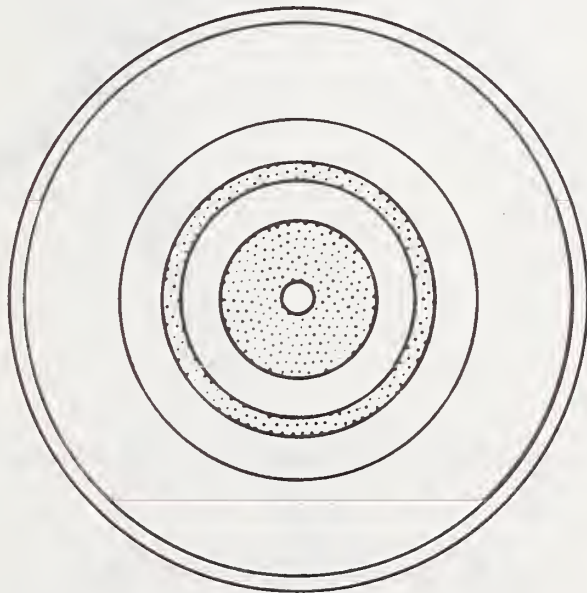
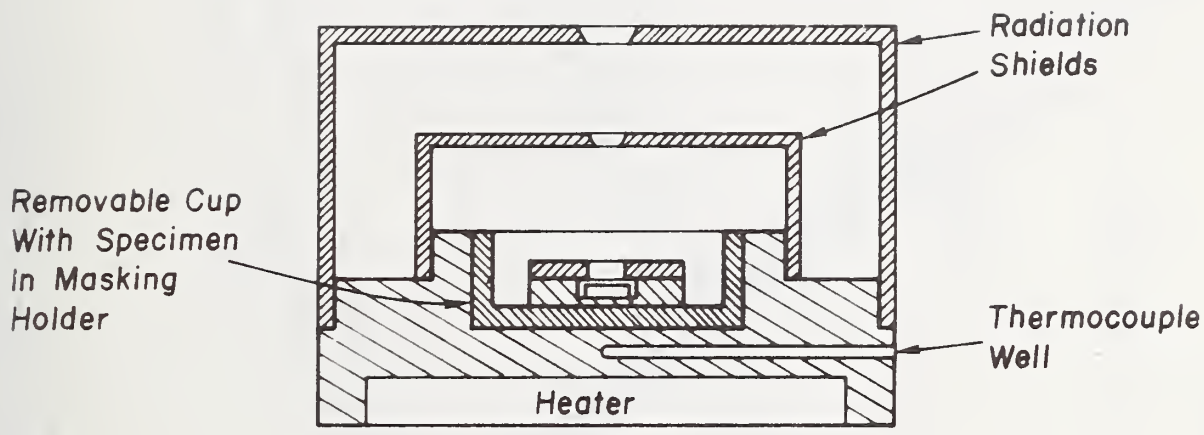
FIGURE CAPTIONS

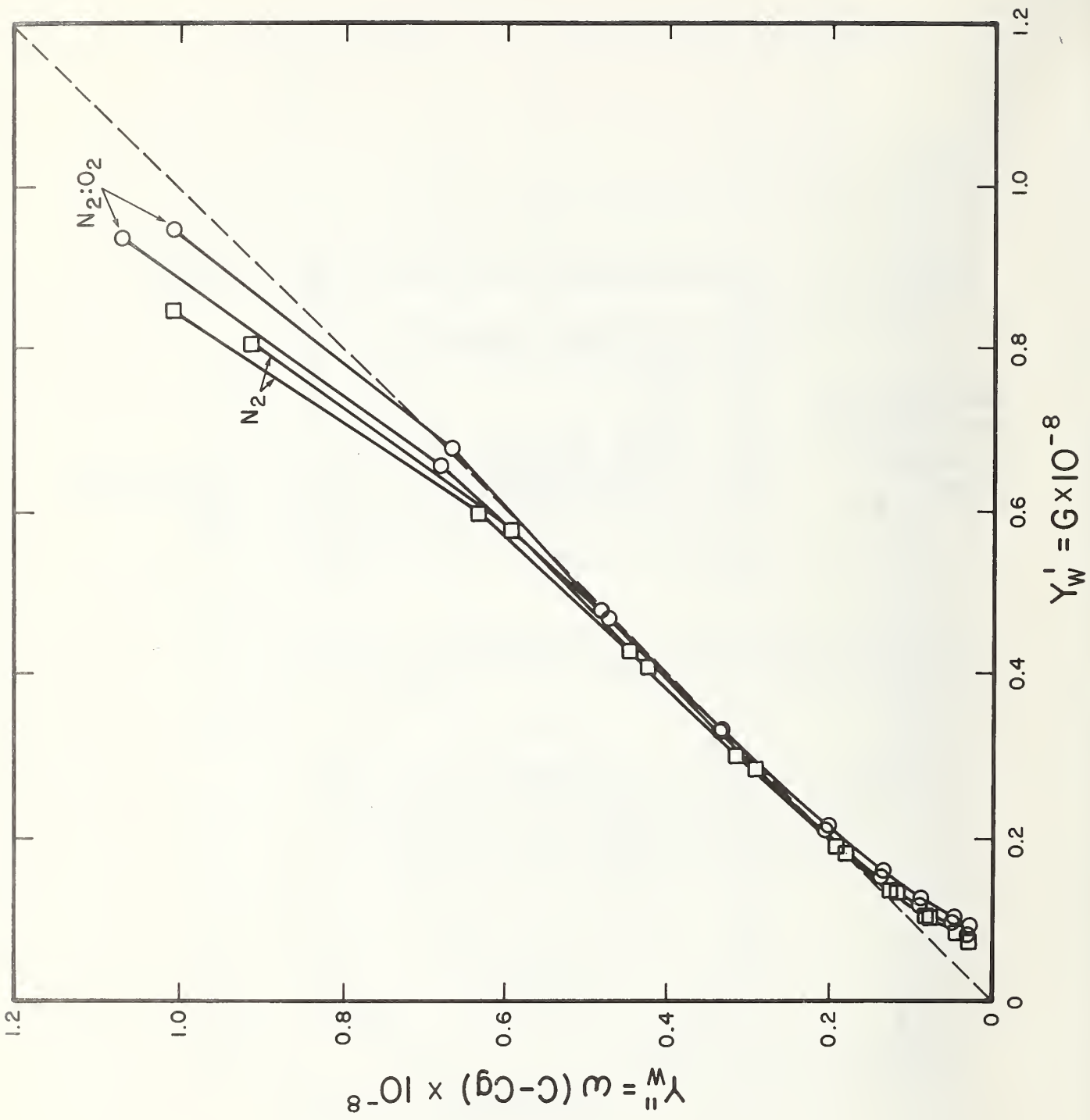
1. Schematic representation of electrolytic cell for crystal growth of $\text{Ca}(\text{OH})_2$. "Reservoir" indicates layer of finely-divided solid $\text{Ca}(\text{OH})_2$.
2. Schematic concentration profiles for OH^- and Ca^{2+} ions during electrolytic crystal growth for transport by OH^- only, Ca^{2+} only, and both OH^- and Ca^{2+} .
3. Jig for radiation shielding of specimen during evaporation of Pt electrodes. Materials is brass. Attachment to cooling coils not shown.
4. Conductance, G , versus $\omega^{1/2}$; and capacitance, C , versus $\omega^{-1/2}$, for 4 sequential runs. The more steeply sloped curves were measured in an $\text{N}_2:\text{O}_2$ (4:1) mixture, whereas the others were measured in N_2 only. The symbol ω denotes the circular frequency.
5. (In text) Equivalent circuits drawn from frequency dependences of G and C ; Fig. 5a. Low frequency; Fig. 5b. Mid-to-high frequency.
6. Complex admittance modified to show the Warburg-like behavior region. $Y'_w = G$ and $Y''_w = \omega(C - C_g)$, where the value of C_g were obtained from high frequency extrapolations of the corresponding capacitance curves shown in Fig. 4.

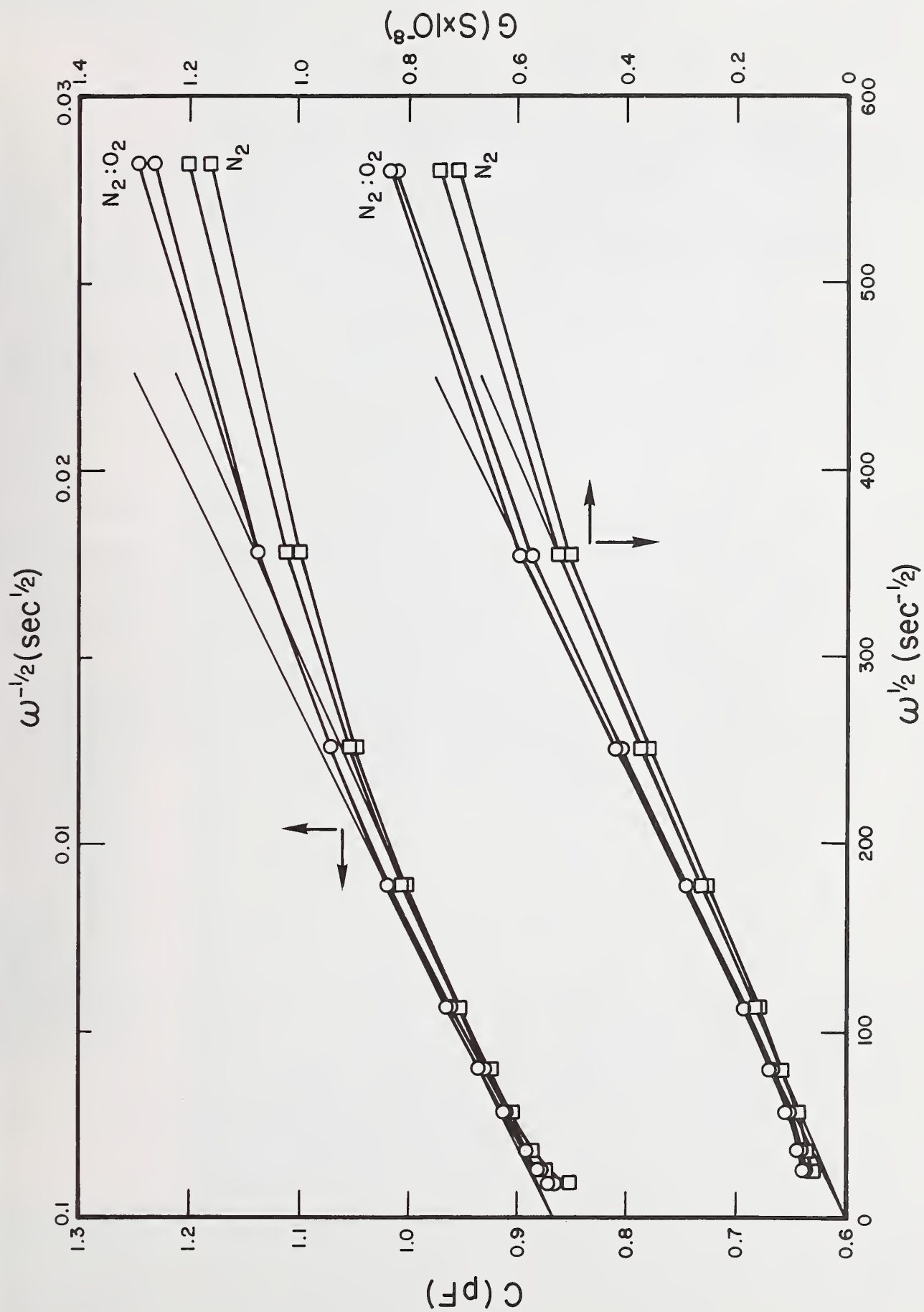


CONCENTRATION RELATIVE TO INITIAL VALUES









U.S. DEPT. OF COMM. BIBLIOGRAPHIC DATA SHEET	1. PUBLICATION OR REPORT NO. NBSIR 74-628	2. Gov't Accession No.	3. Recipient's Accession No.
4. TITLE AND SUBTITLE Mass Transport and Physical Properties of Large Crystals of Calcium Apatites: Studies of Ca(OH) ₂ Crystals for Use in Electrolytic Conversion of Calcium Fluorapatite Crystals to Calcium Hydroxyapatite		5. Publication Date March 1975	6. Performing Organization Code
7. AUTHOR(S) A. D. Franklin and K. F. Young		8. Performing Organ. Report No. NBSIR 74-628	
9. PERFORMING ORGANIZATION NAME AND ADDRESS NATIONAL BUREAU OF STANDARDS DEPARTMENT OF COMMERCE WASHINGTON, D.C. 20234		10. Project/Task/Work Unit No. 3130457	11. Contract/Grant No. Y01-DE-30010
12. Sponsoring Organization Name and Complete Address (Street, City, State, ZIP) National Institute of Dental Research Bethesda, Maryland 20014		13. Type of Report & Period Covered Annual, 9/73 - 8/74	14. Sponsoring Agency Code
15. SUPPLEMENTARY NOTES			
<p>16. ABSTRACT (A 200-word or less factual summary of most significant information. If document includes a significant bibliography or literature survey, mention it here.)</p> <p>In order to convert single crystals of calcium fluorapatite to calcium hydroxyapatite, an electrolytic cell technique will be explored. To utilize such a technique, the cathode compartment must consist of a source of hydroxyl ions and a barrier to the flow of all others. Ca(OH)₂ has been selected for the cathode material, backed by a Pt electrode in an atmosphere containing H₂O and O₂. Ca(OH)₂ crystals have been grown and Ag as well as Pt electrodes applied to them. Their ac admittance as a function of temperature has been measured and analyzed. A Warburg contribution to the admittance was observed to depend upon the presence of O₂. Equivalent circuits have been generated from the data allowing us to tentatively characterize the electrical properties of the electroded crystal system.</p>			
<p>17. KEY WORDS (six to twelve entries; alphabetical order; capitalize only the first letter of the first key word unless a proper name; separated by semicolons)</p> <p>Ac impedance; calcium apatites; calcium hydroxide; crystal growth; electrolysis; interfacial polarization; ionic conduction; mass transport.</p>			
<p>18. AVAILABILITY <input checked="" type="checkbox"/> Unlimited</p> <p><input type="checkbox"/> For Official Distribution. Do Not Release to NTIS</p> <p><input type="checkbox"/> Order From Sup. of Doc., U.S. Government Printing Office Washington, D.C. 20402, SD Cat. No. C13</p> <p><input type="checkbox"/> Order From National Technical Information Service (NTIS) Springfield, Virginia 22151</p>		<p>19. SECURITY CLASS (THIS REPORT)</p> <p>UNCLASSIFIED</p>	<p>21. NO. OF PAGES</p> <p>22</p>
		<p>20. SECURITY CLASS (THIS PAGE)</p> <p>UNCLASSIFIED</p>	<p>22. Price</p>